JOURNAL OF BACTERIOLOGY, Mar. 1996, p. 1289–1294 Vol. 178, No. 5
0021-9193/96/$04.00+0

A Mutational Analysis of the Interaction between FliG and FliM, Two Components of the Flagellar Motor of *Escherichia coli*

DONNA L. MARYKWAS AND HOWARD C. BERG*

Department of Molecular and Cellular Biology, Harvard University, Cambridge, Massachusetts 02138

Received 25 September 1995/Accepted 19 December 1995

The motor that drives the flagellar filament of *Escherichia coli* contains three "switch" proteins (FliG, FliM, and FliN) that together determine the direction of rotation. Each is required, in addition, for flagellar assembly and for torque generation. These proteins interact in the *Saccharomyces cerevisiae* two-hybrid system: FliG interacts with FliM, FliM interacts with itself, and FliM interacts with FliN. The interaction between FliG and FliM has been subjected to mutational analysis. FliG (fused to the GAL4 DNA-binding domain) and FliM (fused to a GAL4 transcription activation domain) together activate transcription of a GAL4-dependent *lacZ* reporter gene. DNA encoding FliG was mutagenized by error-prone amplification with *Taq* polymerase, mutant *fliG* genes were cloned (as DNA-binding domain–*fliG* gene fusions) in *S. cerevisiae* by gap repair of plasmid DNA, and mutants exhibiting an interaction defect were isolated in a two-hybrid screen. The mutations were each mapped to the first, second, or last third of the *fliG* gene by multifragment cloning in vivo and then identified by DNA sequencing. In this way, we identified 18 interaction-defective and 15 silent (non-interaction-defective) *fliG* mutations. Several residues within the middle third of FliG are strongly involved in the FliG-FliM interaction, while residues near the N or C terminus are less important. This clustering, when compared with results of previous studies, suggests that the FliG-FliM interaction plays a central role in switching.

An *Escherichia coli* bacterium swims by a series of runs and tumbles that allows it to locate attractants and avoid repellents, a behavioral phenomenon called chemotaxis. Runs are episodes of steady forward movement that occur when flagellar rotary motors rotate counterclockwise (CCW), causing multiple flagellar filaments to coalesce into a coherent helical bundle that generates thrust. Tumbles are episodes of little net displacement that occur when the motors rotate clockwise (CW), causing the flagellar filaments to separate and move independently. Runs are resumed, but in a new direction chosen at random, when the motors rotate CCW once again. Regulation of motor activity at the level of CW-CCW switching allows the cell to prolong runs when conditions improve and thus to drift towards favorable environments (1).

Components of the motor that control switching (FliG, FliM, and FliN) have been identified by mutations that produce CW-biased or CCW-biased motors that disable chemotaxis (9, 12, 17, 19, 20); the mutant cells are phenotypically nonchemotactic (Che^-). Other mutant alleles of each switch gene produce phenotypically nonmotile (Mot^-) or nonflagellate (Fla^-) bacteria. Pairs of mutant switch genes that suppress each other's mutant defects, with few exceptions, involve Che^- alleles of the opposite rotational bias (17, 19) and so might not reflect, a priori, the restoration of protein contacts within a complex. Nevertheless, all three switch proteins appear to be localized in or near a ring (known as the C ring, since it extends into the cytoplasm) at the base of the flagellar motor (5, 10).

We have found that the switch proteins do indeed interact, when tested pairwise in the absence of other motor components, in a *Saccharomyces cerevisiae* two-hybrid system (14). When two proteins that interact are fused to separate domains of the yeast transcription factor GAL4, interaction between the two proteins reunites the two GAL4 domains in a transcription-competent complex (2, 4). Using this system, we have identified FliG-FliM, FliM-FliM, and FliM-FliN switch protein interactions. In a screen of an *E. coli* library, we also have identified interactions between FliG and FliF (the MS ring protein). Thus, FliG, FliM, and FliN appear to be attached to FliF, in that order (14). Here we present a mutational analysis of FliG and its role in the FliG-FliM interaction.

MATERIALS AND METHODS

Strains, plasmids, primers, and PCR materials. *S. cerevisiae* GGY1::171 (7) is *his3 leu2 gal4 gal80* and contains a chromosomally integrated GAL4-dependent *lacZ* reporter gene. Plasmid pMA424 (7) carries the *HIS3* selectable marker and encodes the GAL4 DNA-binding domain. Plasmid pBD-G^{WT} (14), derived from pMA424, encodes a GAL4 DNA-binding domain–FliG fusion protein. Plasmid pAD-M^{WT} (14) encodes a GAL4 transcriptional activation domain-FliM fusion protein but carries *LEU2*. *E. coli* DH5α was from Bethesda Research Laboratories. Our PCR primers (Table 1) were from Integrated DNA Technologies. PCR was performed in a MiniCycler (MJResearch) with either Amplitaq (Cetus) or recombinant *Pfu* DNA polymerase (BioInsight or Stratagene).

Yeast molecular genetics. The materials and methods used for yeast culture and analysis are reported elsewhere (13). Growth on complete synthetic dropout medium (CSM) lacking histidine (CSM-His), leucine (CSM-Lev), or both (CSM-His-Lev) selected for cells transformed with *HIS3*- and/or *LEU2*-containing plasmid DNA. The FliG and FliM fusion proteins expressed from pBD-G^{WT} and pAD-M^{WT} interacted in strain GGY1::171 (14), thereby restoring GAL4-dependent transcription of the resident *lacZ* reporter gene. Two-hybrid interactions were scored in *S. cerevisiae* on SSX-His-Leu plates (SSX is synthetic medium containing sucrose and X-Gal [5-bromo-4-chloro-3-indolyl-β-D-galactopyranoside], optimized for detection of β-galactosidase activity) and led to the formation of blue colonies.

Mutagenesis. We isolated interaction-defective mutations in *fliG* by combining mutagenic gap repair (15) with two-hybrid screening (4), as described in Fig. 1. We generated a pool of mutant *fliG* genes by PCR with Amplitaq polymerase (Cetus), which is error prone. *fliG* was amplified for 25 cycles with pBD-G^{WT} as a template and primers oGAL70+ and oADHterm, which flank the *fliG* insert in this plasmid. The reaction was performed in 50 μl of 1× buffer (50 mM KCl, 10 mM Tris-HCl [pH 9.0], 0.1% Triton X-100, 0.1 mg of bovine serum albumin per ml) that contained 0.5 ng of template, 12.5 nmol of each deoxynucleoside triphosphate, 20 pmol of each primer, 2.5 U of enzyme, and 0.2 to 0.4 μmol of $MgCl_2$. We linearized and gapped pMA424 by restriction digestion with *Eco*RI and *Bam*HI followed by phenol extraction and ethanol precipitation. GGY1::171 yeast cells already transformed with pAD-M^{WT} were cotransformed with 1 μl (50 ng) of gapped pMA424 and 5 μl (50 ng) of *Taq*-amplified *fliG* PCR product. Transformants were selected on CSM-His-Leu plates at 30°C, lifted onto HA filters (Millipore), and transferred to SSX-His-Leu plates. Color was scored the next day, and light blue colonies of various shades (25 of 588) were chosen for subsequent analysis. Dark blue colonies were not chosen, nor were tan transfor-

* Corresponding author.

TABLE 1. Primers used in this study[a]

Name	Sequence	Gene	Priming site
oGAL132-137 (I)	5′-TCATCGGAAGAGAGTAGT-3′	*GAL4*	394→411
oGAL70+	5′-CTGATTTTTCCTCGAGAAGAC-3′	*GAL4*	208→228
oADHterm (T)	5′-GAGCGACCTCATGCTATACC-3′	*ADH1*	1213→1194
mapoGa (A)	5′-AGATATTCTCGAAACTCG-3′	*fliG*	285→302
mapoGb (B)	5′-CGATAATTTGCGGATGCT-3′	*fliG*	391→374
mapoGc (C)	5′-CTGATGAAAACTCAGCAG-3′	*fliG*	613→630
mapoGd (D)	5′-CTCGAACAGGAACATCTC-3′	*fliG*	711→694
mapoGg (G)	5′-TCTGACCGTCGAGCAA-3′	*fliG*	559→544
mapoGk (K)	5′-ACCATTCTGGTGCATCT-3′	*fliG*	394→410
mapoGm (M)	5′-CGTTGTTCGATGAACGTC-3′	*fliG*	440→457
mapoGn (N)	5′-ACGTTCATCGAACAAC-3′	*fliG*	456→441

[a] Each priming site is indicated relative to position +1 of the respective structural gene. Abbreviated primer names (used to name mapping fragments) are indicated in parentheses.

mants that arose because of the vector-related background discussed previously (13). Plasmid DNA was recovered from each mutant and then retransformed into yeast cells to verify the plasmid dependence of the mutant phenotype. Only 18 of the 25 isolates were plasmid dependent. By sequencing these PCR-generated *fliG* mutants, we found that Amplitaq, under the conditions we used, introduced errors on average once every 280 bases.

Genetic mapping. We mapped our interaction-defective *fliG* mutations by multifragment cloning in vivo. This technique was described in detail earlier for *fliG* mutations 10, 15, and 25 (Fig. 1 and 2 of reference 13). This procedure involved the in vivo construction and testing of reciprocal pairs of chimeric genes, one part mutant (or wild type [WT]) and the other part WT (or mutant), fused to the GAL4 DNA-binding domain. The chimeric genes were created in vivo by the homologous recombination (with linearized pMA424) of multiple overlapping gene fragments derived by PCR, which were introduced together into yeast cells by cotransformation. Since the hybrid genes were constructed in a reporter strain (GGY1::171 transformed with pAD-M^{WT}), their interaction phenotypes were scored directly on indicator plates.

In this way, mutations were mapped to the different parts of the *fliG* gene, which were defined by overlapping fragments named after the PCR primers (Table 1) used for their generation. Mutations were mapped to the first one-third of the *fliG* gene by fragment IB, to the last two-thirds by AT, to the first two-thirds by ID, or to the last one-third by CT. Fragments IB and AT overlap, as do ID and CT. Additional pairs of overlapping fragments (IG with MT, IN with MT, and/or IN with KT) were used when necessary to separate closely linked double mutations or to provide additional mapping data (see Results). An overlap 17 bases in length, the IN-MT overlap, was sufficient to allow efficient recombination in vivo.

Mutant sequence determination. We used existing protocols to sequence double-stranded plasmid DNA (3) and PCR products (18) but with [α-^{33}P]dATP and Sequenase. These PCR products were the partial gene fragments derived for mutation mapping and were cleaned over QIAquick columns (from Qiagen) prior to use. We found errors in the published sequence of *fliG* (16) (GenBank accession number L13243) and have submitted what we believe to be the correct sequence. Our sequenced clone was derived from the original sequenced clone, and upon side-by-side comparison on sequencing gels, both had the same differences from the reported sequence. Comparison of the translated *E. coli* (16) and *Salmonella* (11) *fliG* sequences revealed that the two predicted proteins were virtually identical except for a region of 12 amino acids in the middle. Our DNA sequence when translated was in closer agreement with the predicted *Salmonella* protein. Other investigators have noted similar sequence discrepancies (6).

Protein analysis. Measurements of the specific activity of β-galactosidase were performed as described previously (14). To determine the relative abundance of mutant versus WT fusions of FliG to the GAL4 DNA-binding domain, yeast cell extracts were subject to Western blot (immunoblot) analysis. GGY1::171 cells expressing each fusion protein were grown separately under selection in CSM-His liquid medium. Yeast cells from 10 ml of saturated liquid culture were harvested and then extracted by vortexing in the presence of glass beads (0.45-μm diameter; Sigma) in 0.5 ml of ice-cold resuspension buffer (0.1 M Tris [pH 6.8], 20% glycerol, 1 mM dithiothreitol). The extracts were clarified by centrifugation at 510 × *g*. Control extracts were prepared from untransformed GGY1::171 cells and included on each gel. Ten micrograms of protein from each cell extract was separated by sodium dodecyl sulfate-polyacrylamide gel electrophoresis through 4 to 20% gradient gels (Bio-Rad). The separated proteins were electrotransferred to Hybond-ECL nitrocellulose (Amersham) by using an OWL Horizontal Transblotter (model HEP-1) for 3 h at 0.65 mA/cm^2. The blots were processed with the ECL Western blotting detection system of Amersham. The primary antibody was a polyclonal antibody, raised in a rabbit, to the DNA-binding domain of GAL4 (a gift from Steven Passmore). This antibody was preadsorbed with an acetone powder of GGY1::171 cells, prepared as described by Harlow and Lane (8), and then used at a 1:2,000 dilution. The secondary

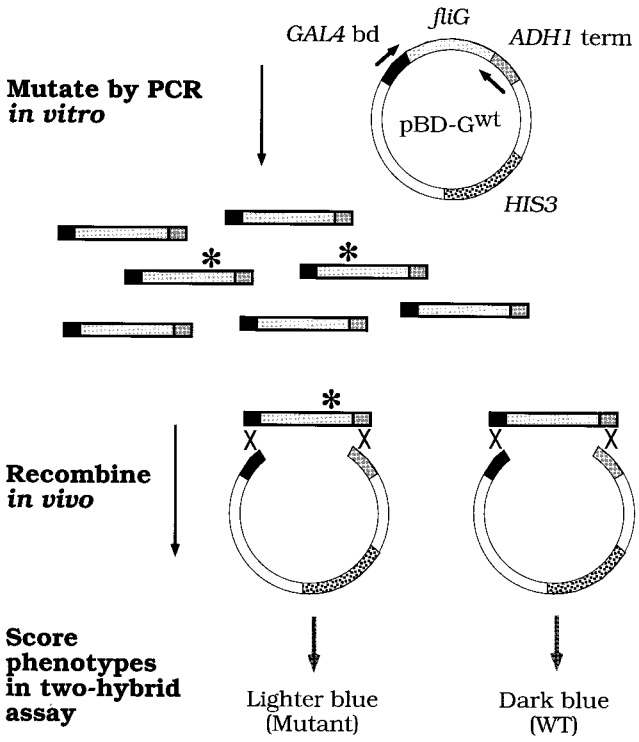

FIG. 1. Procedure to isolate interaction-defective mutations in *fliG*. *fliG* was mutagenized in vitro by PCR with *Taq* polymerase, as described in Materials and Methods. The *fliG*-containing template was plasmid pBD-G^{WT}. PCR with primers (represented by arrows) that flanked the *fliG* insert of this plasmid produced a collection of *fliG* genes, some mutant and some WT, with homology on each end to plasmid DNA. The PCR-generated mutations are represented by asterisks. The regions of homology to plasmid DNA are represented by darker shades. Plasmid pMA424, the GAL4 DNA-binding domain vector from which pBD-G^{WT} was derived, was digested with restriction enzymes to produce linear plasmid DNA with terminal homology to the *fliG*-containing PCR products. Introduced together into yeast strain GGY1::171::pAD-M^{WT}, these DNAs underwent in vivo homologous recombination, represented by X. Each recombinant plasmid thus created transformed *S. cerevisiae* to histidine prototrophy and encoded a GAL4 DNA-binding domain–FliG fusion protein. Two-hybrid interactions with the WT GAL4 activation domain-FliM fusion (encoded by resident plasmid pAD-M^{WT}) were scored on X-Gal-containing indicator plates. WT interactions were dark blue, whereas defective interactions were lighter blue.

TABLE 2. Properties of *fliG* mutants that exhibit FliG-FliM interaction defects

fliG allele[a]	*lacZ* expression[b]	Map location[c]	Map data or reference[d]	Mutation(s)[e]: Within map location	Mutation(s)[e]: Outside map location
1	0.125	ID-CT overlap	IB^{1} + AT^{WT} (100% DB), IB^{WT} + AT^{1} (100% LB), ID^{1} + CT^{WT} (97.5% DB, 2.5% LB), ID^{WT} + CT^{1} (41.6% DB, 58.4% LB)	**GAG→GTG = Glu-232→Val**	GAC→GTC = Asp-243→Val, AAA→GAA = Lys-273→Glu
2	0.077	ID-CT overlap	IB^{2} + AT^{WT} (97% DB, 3% LB), IB^{WT} + AT^{2} (100% LB), ID^{2} + CT^{WT} (39% DB, 61% LB), ID^{WT} + CT^{2} (47.6% DB, 52.4% LB)	**CTG→CCG = Leu-225→Pro**	
3	0.111	ID-CT overlap	IB^{3} + AT^{WT} (83.3% DB, 16.7% LB), IB^{WT} + AT^{3} (3.4% DB, 96.6% LB), ID^{3} + CT^{WT} (34.1% DB, 65.9% LB), ID^{WT} + CT^{3} (71.7% DB, 28.3% LB)	**CAG→CGG = Gln-210→Arg**	TGA→CGA = Opa-332→Arg
4	0.500	IB-AT overlap	IB^{4} + AT^{WT} (48.4% DB, 51.6% LB), IB^{WT} + AT^{4} (43.2% DB, 56.8% LB), ID^{4} + CT^{WT} (31.6% DB, 68.4% LB), ID^{WT} + CT^{4} (96.6% DB, 3.4% LB)	**ATG→ACG = Met-113→Thr**	GAG→GGG = Glu-58→Gly
5	0.250	ID-CT overlap	IB^{5} + AT^{WT} (100% DB), IB^{WT} + AT^{5} (100% LB), ID^{5} + CT^{WT} (60.5% DB, 39.5% LB), ID^{WT} + CT^{5} (72.4% DB, 27.6% LB)	**GCC→ACC = Ala-217→Thr**	
6	0.063	Middle third	IB^{6} + AT^{WT} (100% DB), IB^{WT} + AT^{6} (100% LB), ID^{6} + CT^{WT} (7.9% DB, 92.1% LB), ID^{WT} + CT^{6} (95.7% DB, 4.3% LB)	**TTG→TCG = Leu-159→Ser**	GAA→GTA = Glu-108→Val, GAT→GTT = Asp-241→Val
10	0.007	Middle third	13	**CTG→CCG = Leu-153→Pro**	CAA→CGA = Gln-141→Arg, GTG→GCG = Val-25→Ala
12	0.200	Last third (CT)	IB^{12} + AT^{WT} (100% DB), IB^{WT} + AT^{12} (4.3% DB, 95.7% LB), ID^{12} + CT^{WT} (97.2% DB, 2.8% LB), ID^{WT} + CT^{12} (100% LB)	**GTG→GAG = Val-312→Glu**	
13	0.167	Middle third	IB^{13} + AT^{WT} (100% DB), IB^{WT} + AT^{13} (100% LB), ID^{13} + CT^{WT} (100% LB), ID^{WT} + CT^{13} (99.3% DB, 0.7% LB)	**GTA→TTA = Val-178→Leu**	
14	0.071	Middle third	IB^{14} + AT^{WT} (100% DB), IB^{WT} + AT^{14} (100% LB), ID^{14} + CT^{WT} (0.5% DB, 99.5% LB), ID^{WT} + CT^{14} (99.8% DB, 0.2% LB)	**ACC→TCC = Thr-132→Ser,** GGC→AGC = Gly-195→Ser	
15	0.043	ID-CT overlap	13	**CTG→CCG = Leu-225→Pro**	
16	0.063	ID-CT overlap	IB^{16} + AT^{WT} (97.4% DB, 2.6% LB), IB^{WT} + AT^{16} (100% LB), ID^{16} + CT^{WT} (52.4% DB, 47.6% LB), ID^{WT} + CT^{16} (38.4% DB, 61.6% LB)	**ATC→ACC = Ile-229→Thr**	GTC→GCC = Val-331→Ala
17	0.167	Middle third	IB^{17} + AT^{WT} (97.7% DB, 2.3% LB), IB^{WT} + AT^{17} (100% LB), ID^{17} + CT^{WT} (8.4% DB, 91.6% LB), ID^{WT} + CT^{17} (96.7% DB, 3.3% LB)	**GTG→GCG = Val-157→Ala**	
19	0.071	Middle third	IB^{19} + AT^{WT} (98.5% DB, 1.5% LB), IB^{WT} + AT^{19} (16.7% DB, 83.3% LB), ID^{19} + CT^{WT} (100% LB), ID^{WT} + CT^{19} (91.7% DB, 8.3% LB)	**ATT→CTT = Ile-129→Leu,** GTG→GCG = Val-196→Ala	CAG→CGG = Gln-51→Arg, ATC→GTC = Ile-229→Val
21	0.003	Middle third	IB^{21} + AT^{WT} (100% DB), IB^{WT} + AT^{21} (100% LB), ID^{21} + CT^{WT} (100% LB), ID^{WT} + CT^{21} (98.6% DB, 1.4% LB)	**CTG→CAG = Leu-146→Gln,** AAC→GAC = Asn-204→Asp	CTC→CCC = Leu-29→Pro
22	0.111	Middle third	IB^{22} + AT^{WT} (99.5% DB, 0.5% LB), IB^{WT} + AT^{22} (76.8% DB, 23.2% LB), ID^{22} + CT^{WT} (57.9% DB, 42.1% LB), ID^{WT} + CT^{22} (98.7% DB, 1.3% LB)	**GTG→GCG = Val-135→Ala**	
23	0.125	Middle third	IB^{23} + AT^{WT} (100% DB), IB^{WT} + AT^{23} (3% DB, 97% LB), ID^{23} + CT^{WT} (0.5% DB, 99.5% LB), ID^{WT} + CT^{23} (98.3% DB, 1.7% LB)	**GTG→GCG = Val-157→Ala**	
25	0.002	Middle third	13	**CAC→CCC = His-155→Pro**	

[a] Mutant alleles of *fliG* that produced a FliG-FliM two-hybrid interaction defect were isolated as outlined in Fig. 1.

[b] The WT FliG-FliM two-hybrid interaction is represented by the level of reporter gene expression in GGY1::171 cotransformed with pBD-G^{WT} and pAD-M^{WT}. *fliG* mutants (derivatives of plasmid pBD-G^{WT}) were isolated, and their interaction defects (reduced reporter gene expression levels) were measured. The specific activity of β-galactosidase is reported as the fraction of the WT level.

[c] Deduced map locations are based solely on data in this table.

[d] Mutant alleles of *fliG* that produced a FliG-FliM two-hybrid interaction defect were dissected genetically by multifragment cloning in vivo (13) to map the mutations of interest. Mutant IB fragments were recombined with AT^{WT}. Mutant AT fragments were recombined with IB^{WT}. Mutant ID fragments were recombined with CT^{WT}. Mutant CT fragments were recombined with ID^{WT}. For each pair of mutant and WT fragments so joined, an average of 143 recombinants were scored, and results are reported as the percentage of the total number of recombinants that displayed each phenotype. DB, dark blue; LB, light blue.

[e] For each *fliG* allele, DNA sequence analysis revealed a mutation(s) within the deduced map location. In some cases, mutations outside the deduced map location were also identified. Interaction-defective mutations, on the basis of all of the data presented in this paper, are in boldface.

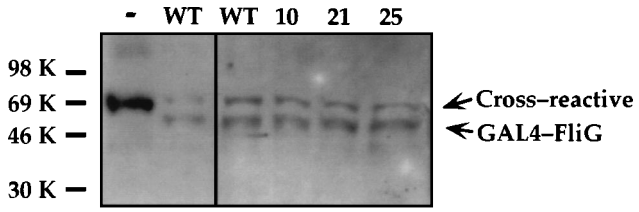

FIG. 2. Western blot analysis of interaction-defective mutants. Each mutant FliG fusion protein was examined for length and abundance, as described in Materials and Methods. Representative data for mutants 10, 21, and 25, compared with the WT FliG fusion protein, are shown. Antibodies against the GAL4 DNA-binding domain cross-reacted with a protein expressed in yeast strain GGY1::171; an overloaded example, as a negative control (−), is shown. In addition to this cross-reactive species, a protein with the expected molecular mass (55.6 kDa) was detected in GGY1::171 cells expressing either the WT or mutant GAL4-FliG fusion protein. The position of each protein standard is indicated to the left, with sizes indicated in kilodaltons (K).

antibody, horseradish peroxidase-labeled anti-rabbit immunoglobulin, was similarly preadsorbed and used at a 1:1,000 dilution. Multiple exposures to Kodak XAR film, usually ranging in time from 1 to 15 min, were made.

Nucleotide sequence accession number. The *fliG* sequence determined in this study has been submitted to GenBank (accession number U46011).

RESULTS

Isolation of interaction-defective mutations in *fliG*. We have recently identified several two-hybrid interactions between the three proteins that make up the switch of the *E. coli* flagellar motor (14). One of the strongest interactions was between FliG and FliM. Coexpression, in *S. cerevisiae*, of FliG (fused to the GAL4 DNA-binding domain) and FliM (fused to a GAL4 activation domain) activated transcription of a GAL4-dependent *lacZ* reporter gene. FliG and FliM interacted in yeast cells in the absence of other *E. coli* motor components. To better understand this FliG-FliM interaction, we generated mutations that destroyed it. Figure 1 illustrates the method used to isolate interaction-defective mutations in *fliG*. Details of the mutagenesis are given in Materials and Methods. In brief, by using the DNA-binding domain gene fusion to WT *fliG* as a template (pBD-G^{WT}) and PCR with error-prone *Taq* polymerase, we generated a pool of mutant *fliG* genes that retained homology at both ends to plasmid pMA424, the GAL4 DNA-binding domain vector. Plasmid pMA424 was linearized to create free ends available for homologous recombination. This linear vector and the pool of *fliG* inserts, cotransformed into yeast cells, were recombined in vivo. The activation domain fusion to FliM and the reporter gene were already present in the yeast cells, allowing direct screening for lighter blue transformants.

Of 588 transformants screened, we obtained 18 FliG mutants that appeared to interact less well with FliM. The severity of the mutations varied over a wide range, as indicated by in vitro β-galactosidase measurements (Table 2). For example, FliG mutant 4 resulted in only a twofold reduction in reporter gene expression, whereas FliG mutant 25 resulted in a greater than 500-fold reduction. Each mutant FliG fusion protein appeared to be of full length and to be expressed at a steady-state level comparable to that of the WT fusion protein, as judged by Western blots probed with antiserum to the GAL4 DNA-binding domain. Representative data are shown in Fig. 2. Hence, the mutant phenotype appears to be due to specific amino acid substitutions that interfere with the FliG-FliM interaction and not to a reduction in the amount of protein.

Mapping the interaction-defective mutations in *fliG*. We mapped our interaction-defective *fliG* mutations by multifragment cloning in vivo, as described previously (13). *fliG* was divided into thirds defined by the overlapping fragments IB (first one-third) and AT (last two-thirds) or ID (first two-thirds) and CT (last one-third). These overlapping fragments were derived by PCR. For each mutant, a standard set of four chimeric gene fusions, part mutant and part WT, was constructed (and tested) in vivo to map the interaction-defective mutation to the first, second, or last third of the mutant *fliG* gene. The mapping data for *fliG* mutants 10, 15, and 25 were used to illustrate this technique (13), so they will not be duplicated here. The (standard set of) mapping data for the remaining interaction-defective *fliG* mutants are shown in Table 2. Some map locations (mutations 3, 4, and 22) were confirmed by the construction and testing of additional pairs of reciprocal hybrids (Table 3). As was the case for *fliG* mutation 15 (13), *fliG* mutations 1, 2, 5, and 16 clearly mapped to the region of overlap between ID and CT. Mutation 12 was the

TABLE 3. Refined mapping data

fliG allele	Map location[a]	Map data[b]	Mutation[c]	
			Interaction-defective	Silent
3	Not IG	IG^{3} + MT^{WT} (96.4% DB, 3.6% LB), IG^{WT} + MT^{3} (2% DB, 98% LB), IN^{3} + MT^{WT} (95.8% DB, 4.2% LB), IN^{WT} + MT^{3} (6.4% DB, 93.6% LB)	CAG→CGG = Gln-210→Arg	
4	Not MT	IG^{4} + MT^{WT} (1.5% DB, 98.5% LB), IG^{WT} + MT^{4} (99% DB, 1% LB), IN^{4} + MT^{WT} (3% DB, 97% LB), IN^{WT} + MT^{4} (98% DB, 2% LB)	ATG→ACG = Met-113→Thr	
14	Not MT	IN^{14} + MT^{WT} (8.2% DB, 91.8% LB), IN^{WT} + MT^{14} (95.2% DB, 4.8% LB)	ACC→TCC = Thr-132→Ser	GGC→AGC = Gly-195→Ser
19	Not KT	IN^{19} + KT^{WT} (2% DB, 98% LB), IN^{WT} + KT^{19} (99.5% DB, 0.5% LB)	ATT→CTT = Ile-129→Leu	GTG→GCG = Val-196→Ala
21	Not MT	IG^{21} + MT^{WT} (0.6% DB, 99.4% LB), IG^{WT} + MT^{21} (99% DB, 1% LB)	CTG→CAG = Leu-146→Gln	AAC→GAC = Asn-204→Asp
22	Not MT	IN^{22} + MT^{WT} (51.9% DB, 48.1% LB), IN^{WT} + MT^{22} (96.6% DB, 3.4% LB)	GTG→GCG = Val-135→Ala	

[a] Deduced map locations are based solely on data in this table.

[b] IG fragments were recombined with MT fragments, IN fragments were recombined with MT fragments, or IN fragments were recombined with KT fragments. For each pair of mutant and WT fragments so joined, an average of 304 recombinants were scored, and results are reported as the percentage of the total number of recombinants that displayed each phenotype. DB, dark blue; LB, light blue.

[c] Mutations were classified as interaction-defective or silent, on the basis of combined data from this table and Table 2.

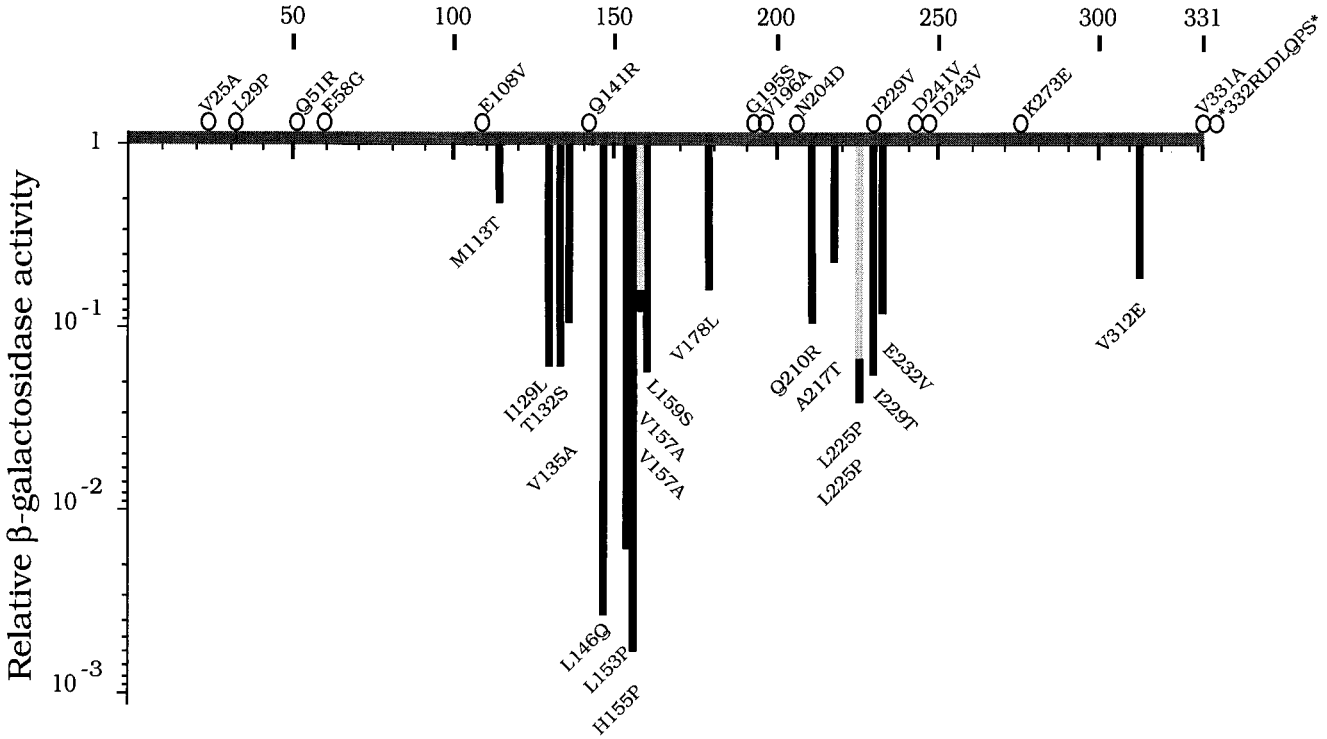

FIG. 3. FliG-FliM two-hybrid interaction defects produced by amino acid substitutions throughout FliG. The horizontal bar, from left to right, represents the FliG protein from the N to the C terminus. Amino acid substitutions are indicated in the one-letter code. Silent amino acid substitutions are indicated by open circles. Amino acid substitutions that produced interaction defects are indicated by vertical bars that represent the amount of β-galactosidase specific activity produced by each mutant, relative to that of WT FliG, in FliG-FliM interaction assays. Substitutions found more than once are indicated by two-toned bars, with the data for one isolate indicated by the length of the light segment and those for an independent isolate indicated by the combined length of the light and dark segments. This figure summarizes the data of Tables 2 and 3.

only mutation that mapped to the last third of *fliG*. The remaining mutations clearly mapped to the middle third of the *fliG* gene.

The mapped mutations were identified by sequencing (Tables 2 and 3). Most mutants had only one base change in the map location identified by the standard set of four in vivo tests. However, as was the case for *fliG* mutant 10 (13), two missense mutations were discovered in the map locations for *fliG* mutants 14, 19, and 21. In each case, the two base changes were physically separated and independently tested by the in vivo construction and analysis of a third pair of reciprocal hybrids. These separation data are given in Table 3. In the case of mutant 14, the Thr-132→Ser substitution was defective, whereas the Gly-195→Ser substitution was silent. Similarly, for *fliG* mutant 19, the Ile-129→Leu substitution was defective, whereas Val-196→Ala was silent. For *fliG* mutant 21, the Leu-146→Gln substitution was defective, but Asn-204→Asp was silent.

Identification of silent *fliG* mutations. For many of our *fliG* mutants, we sequenced more than just the genetically identified map segment. Base changes found outside the mapped location of a given mutation (Tables 2 and 3) were, by definition, silent; they had no detectable effect upon the gene function assayed, the FliG-FliM two-hybrid interaction.

DISCUSSION

FliG and the FliG-FliM interaction. We first found that FliG fused to GAL4's DNA-binding domain and FliM fused to GAL4's transcription activation domain, when coexpressed in yeast cells, reconstituted an activator of GAL4-dependent *lacZ* reporter gene expression (14). We then generated a collection of plasmid-borne FliG mutants (fused to the DNA-binding domain) that interact with FliM less well than does WT FliG. This mutational analysis has most likely revealed FliG residues that contact FliM. The mutant GAL4-FliG fusion proteins were synthesized in yeast cells and maintained at levels comparable to those of the WT fusion protein. Moreover, even severe interaction defects (for example, those due to amino acid substitutions L-225→P [L225P] and H155P of mutants 15 and 25, respectively) were genetically suppressible by compensating changes in FliM fused to the GAL4 activation domain (14a). Thus, it is unlikely that the mutant GAL4-FliG fusion proteins were simply denatured, in which case they would not be suppressible. All interaction defects were traced to single amino acid substitutions.

The results of our *fliG* mutational analysis are summarized in Fig. 3. The histogram highlights the distribution and relative importance of the *fliG* mutations that we found. The longer the bar, the more severe the mutation, the weaker the FliG-FliM interaction, and thus the lower the levels of reporter gene expression. Silent changes are shown as open circles. Most of the important changes are located in the middle third of the gene and are new, heretofore unidentified, mutations. One exception is the T132S substitution, which was previously isolated as a *cheY* suppressor and shown to be CW biased (9). Substitutions V135A, V178L, and A217T, although new, affect residues identified as important in previous studies (9): A217P was shown to cause the Mot$^-$ phenotype, V135F was CW biased, and V135L and V178E were each CCW biased.

Two of our silent mutations are associated with mutant phenotypes identified in previous screens. The K273E substitution is identical to a previously identified Mot$^-$ allele of *fliG* in *Salmonella typhimurium* (9), but it is silent in our assay and therefore not important for the FliG-FliM interaction. Similarly, our silent G195S substitution is identical to a previously identified CW-biased allele of *fliG* (9). Residue 108 is the site of our silent E108V substitution and the previously identified CW-biased E108K substitution (9); E108K also suppresses mutant *motB* (6).

The distribution of the bars in Fig. 3 suggests that neither the N nor C terminus of FliG is important for the FliG-FliM interaction. Indeed, we have found that the N-terminal 45 amino acids can be removed with little effect (as in the fusion encoded by plasmid pGBT9-fliG$^{\Delta 1-45}$ [14]). Interestingly, very few Che$^-$ alleles of *fliG* have been found close to these termini. Instead, they are mostly located throughout the middle third of the gene, much of which can be deleted without affecting flagellar assembly (9). Moreover, the largest cluster of Mot$^-$ *fliG* alleles is located in the last quarter of the gene, between residues 236 and 262 (9), where we found very few changes that resulted in a defect in the FliG-FliM interaction.

Preliminary observations suggest that most of our interaction-defective *fliG* mutations permit flagellar assembly and rotation. Of the eight mutants examined so far, only two were Mot$^-$, although they were flagellated. Synthesis, but not rotation, of flagella also was supported by the mutant FliG protein missing 45 N-terminal amino acids (encoded by pGBT9-fliG$^{\Delta 1-45}$), which nevertheless interacted well with FliM but not FliF (14). The Mot$^-$ defect of this mutant was thus most likely due to impaired contact between FliG and FliF. All of these facts taken together suggest that the FliG-FliM interaction is not primarily involved in flagellar assembly or motor rotation but instead might play a critical role in switching.

ACKNOWLEDGMENTS

We thank Steven Passmore for the gift of anti-GAL4 DNA-binding domain antibodies, for expert graphic artistry, and for helpful comments on the manuscript.

This work was supported by Public Health Service grant AI16478 and National Science Foundation grant MCB-9213011.

REFERENCES

1. **Berg, H. C.** 1988. A physicist looks at bacterial chemotaxis. Cold Spring Harbor Symp. Quant. Biol. **53:**1–9.
2. **Chien, C.-T., P. L. Bartel, R. Sternglanz, and S. Fields.** 1991. The two-hybrid system: a method to identify and clone genes for proteins that interact with a protein of interest. Proc. Natl. Acad. Sci. USA **88:**9578–9582.
3. **Del Sal, G., G. Manfioletti, and C. Schneider.** 1989. The CTAB-DNA precipitation method: a common mini-scale preparation of template DNA from phagemids, phages or plasmids suitable for sequencing. BioTechniques **7:**514–519.
4. **Fields, S., and O.-K. Song.** 1989. A novel genetic system to detect protein-protein interactions. Nature (London) **340:**245–246.
5. **Francis, N. R., G. E. Sosinsky, D. Thomas, and D. J. DeRosier.** 1994. Isolation, characterization and structure of bacterial flagellar motors containing the switch complex. J. Mol. Biol. **235:**1261–1270.
6. **Garza, A. G., L. W. Harris-Haller, R. A. Stoebner, and M. D. Manson.** 1995. Motility protein interactions in the bacterial flagellar motor. Proc. Natl. Acad. Sci. USA **92:**1970–1974.
7. **Gill, G., and M. Ptashne.** 1987. Mutants of GAL4 protein altered in an activation function. Cell **51:**121–126.
8. **Harlow, E., and D. Lane.** 1988. Antibodies: a laboratory manual. Cold Spring Harbor Laboratory Press, Cold Spring Harbor, N.Y.
9. **Irikura, V. M., M. Kihara, S. Yamaguchi, H. Sockett, and R. M. Macnab.** 1993. *Salmonella typhimurium fliG* and *fliN* mutations causing defects in assembly, rotation, and switching of the flagellar motor. J. Bacteriol. **175:** 802–810.
10. **Khan, I. H., T. S. Reese, and S. Khan.** 1992. The cytoplasmic component of the bacterial flagellar motor. Proc. Natl. Acad. Sci. USA **89:**5956–5960.
11. **Kihara, M., M. Homma, K. Kutsukake, and R. M. Macnab.** 1989. Flagellar switch of *Salmonella typhimurium*: gene sequences and deduced protein sequences. J. Bacteriol. **171:**3247–3257.
12. **Magariyama, Y., S. Yamaguchi, and S. Aizawa.** 1990. Genetic and behavioral analysis of flagellar switch mutants of *Salmonella typhimurium*. J. Bacteriol. **172:**4359–4369.
13. **Marykwas, D. L., and S. E. Passmore.** 1995. Mapping by multifragment cloning *in vivo*. Proc. Natl. Acad. Sci. USA **92:**11701–11705.
14. **Marykwas, D. L., S. A. Schmidt, and H. C. Berg.** 1996. Interacting components of the flagellar motor of *Escherichia coli* revealed by the two-hybrid system in yeast. J. Mol. Biol. **256:**564–576.

14a. **Marykwas, D. L., A. H. Wong, and H. C. Berg.** Unpublished data.

15. **Muhlrad, D., R. Hunter, and R. Parker.** 1992. A rapid method for localized mutagenesis of yeast genes. Yeast **8:**79–82.
16. **Roman, S. J., B. B. Frantz, and P. Matsumura.** 1993. Gene sequence, overproduction, purification and determination of the wild-type level of the *Escherichia coli* flagellar switch protein FliG. Gene **133:**103–108.
17. **Sockett, H., S. Yamaguchi, M. Kihara, V. M. Irikura, and R. M. Macnab.** 1992. Molecular analysis of the flagellar switch protein FliM of *Salmonella typhimurium*. J. Bacteriol. **174:**793–806.
18. **Thein, S. L.** 1989. A simplified method of direct sequencing of PCR amplified DNA with Sequenase T7 DNA polymerase. Comments **16:**8.
19. **Yamaguchi, S., S. Aizawa, M. Kihara, M. Isomura, C. J. Jones, and R. M. Macnab.** 1986. Genetic evidence for a switching and energy-transducing complex in the flagellar motor of *Salmonella typhimurium*. J. Bacteriol. **168:**1172–1179.
20. **Yamaguchi, S., H. Fujita, A. Ishihara, S. Aizawa, and R. M. Macnab.** 1986. Subdivision of flagellar genes of *Salmonella typhimurium* into regions responsible for assembly, rotation, and switching. J. Bacteriol. **166:**187–193.